GRAVITY MODELING THEORY

The gravity method as it is applied in exploration is fundamentally governed by Newton's universal law of attraction. The force caused by the underlying mass of the Earth at a given location on the mass inside the gravimeter is being measured[1]. Horizontal variations of density within the subsurface thereby cause variations in the measured gravity field. The method is quite useful in identifying the regional architecture of the Earth's crust – identifying regions of interest for resource exploration.

The gravitational force resulting from a point source can be described using the following equations.

$$\overrightarrow{F_g} = \frac{\partial U}{\partial r} = -G\frac{m}{r^2}\left(\frac{\vec{\boldsymbol{r}}}{r}\right)$$

$$= F_x\hat{e}_x + F_y\hat{e}_y + F_z\hat{e}_z$$

Where $\overrightarrow{F_g}$ is the gravitational force, U is the gravitational potential, G is the universal gravitational constant (equal to 6.67 x 10^{-11} $m^3/kg \cdot s^2$), m is the mass of the point source, and $\vec{\boldsymbol{r}}$ is the vector between the measurement station and the point source. The gravimeter employed in this survey measures the vertical component of the gravitational force, g_z.

$$\frac{\partial U}{\partial z} = g_z = -G\frac{m\,\Delta z}{r^3}$$

Δz, above, is the vertical distance between the observation point and the point source. The gravimeter however, is not measuring a point source but a multitude of mass bodies. The physical property being measured is then mass per unit volume (or the density, ρ) of a source body. By considering density and integrating over the lower-a and upper-b limits of each dimension of a 3D source, the gravitational potential and its associated vertical component of gravity at location *(x, y, z)* for a source at location *(x', y', z')* become

$$U(x,y,z) = \int_{z'_a}^{z'_b}\int_{y'_a}^{y'_b}\int_{x'_a}^{x'_b} G\frac{\rho}{r}\partial x'\partial y'\partial z'$$

$$g_z = \int_{z'_a}^{z'_b}\int_{y'_a}^{y'_b}\int_{x'_a}^{x'_b} -G\frac{\rho\,\Delta z}{r^3}\partial x'\partial y'\partial z'$$

---

[1] This statement ignores unwanted effects which may be present in the data, including those related to variations in position, elevation, speed of the gravimeter, geologic noise, and aliasing.

For 2D modeling with infinite strike-length along the y-axis, the vertical component of the gravitational field of a 2D source reduces to

$$g_z = \int_{z'_a}^{z'_b} \int_{x'_a}^{x'_b} \left\{ \frac{\partial U'}{\partial z} = -2G \frac{\Delta z}{r^2} \rho \right\} \partial x' \partial z'$$

(Hubbert, 1948) showed that a gravimetric effect of two-dimensional masses can be calculated using a line-integral method. The gravity anomaly Δg, at the origin of the coordinates (the observation point) produced by a density contrast of $\Delta\rho$ may be calculated. First, consider representing the source mass body as a series of $\Delta z \Delta\theta$ solenoids. If the solenoids are small enough such that their density may be considered constant, the contribution to gravity of a single solenoid, and subsequently the integration over any area can be approximated by

$$\Delta g = 2G\, \rho\, \Delta\theta\, \Delta z$$

$$g = 2G \int \int \rho \, d\theta \, dz = 2G \sum_{i=1}^{i=n} \rho_i \, \Delta\theta \, \Delta z$$

Where *n* is the number of solenoids in the area. This method is shown in Figure 1 visually.

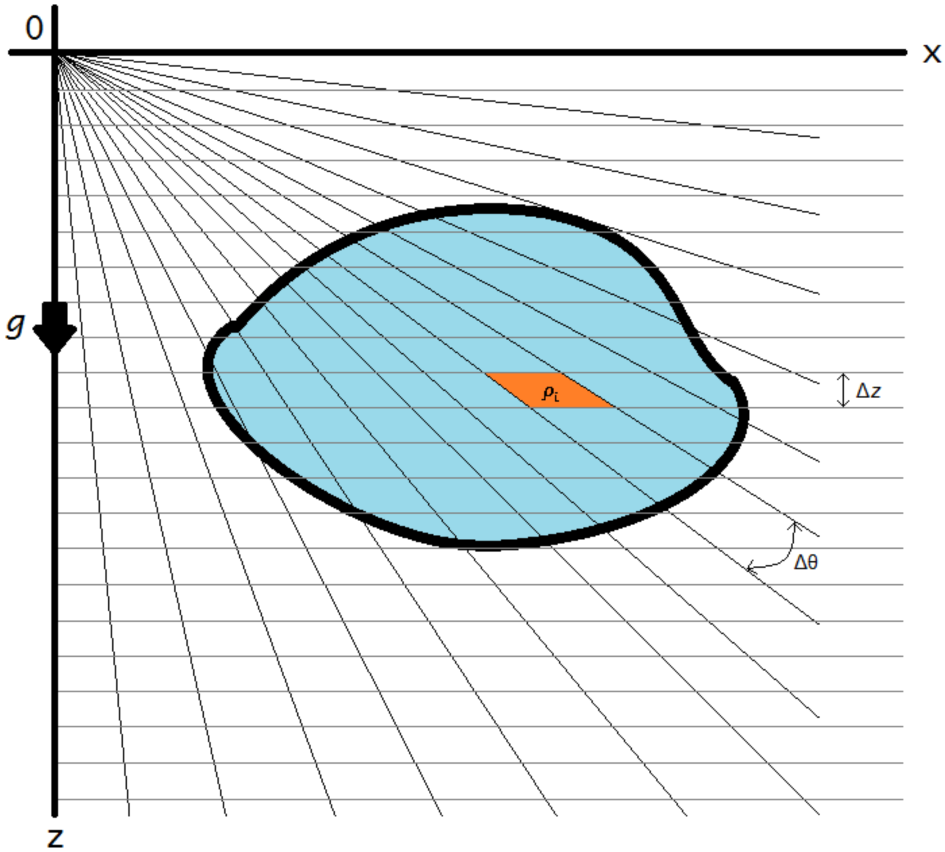

Figure 1: The calculation of a gravity anomaly resulting from a mass body source (blue) through areal integration of $d\theta dz$-solenoids, modified from Hubbert, 1948.

For a single solenoid $d\theta dz$, which is surrounded by lines θ, $\theta+d\theta$, z, and $z+dz$, consider its line integral $\oint \theta\, dz$. This is shown below in Figure 2.

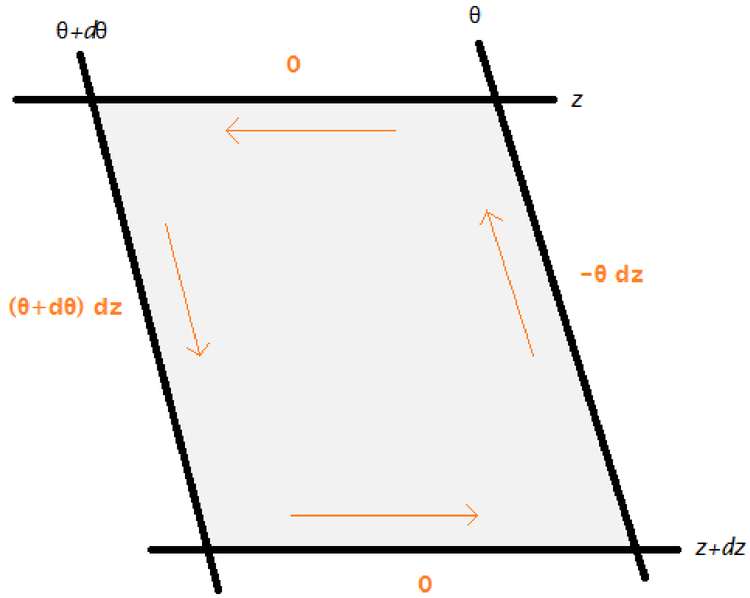

$$\oint \theta\, dz = 0 + (\theta + d\theta)dz + 0 - \theta\, dz$$
$$= d\theta\, dz$$

Figure 2: The line integral about a single dθdz-solenoid, modified from (Hubbert, 1948).

Over a finite area S (containing many solenoids), we may then calculate $\iint d\theta\, dz$ by integrating over the area of line-integrals as given by the following equation.

$$\int\int_S d\theta\, dz = \int\int_S \left[\oint \theta\, dz\right]$$

For a source mass body, each interior solenoid path is traversed once in each direction (canceling each other out); however, exterior solenoid paths are traversed only once and always in the same direction.

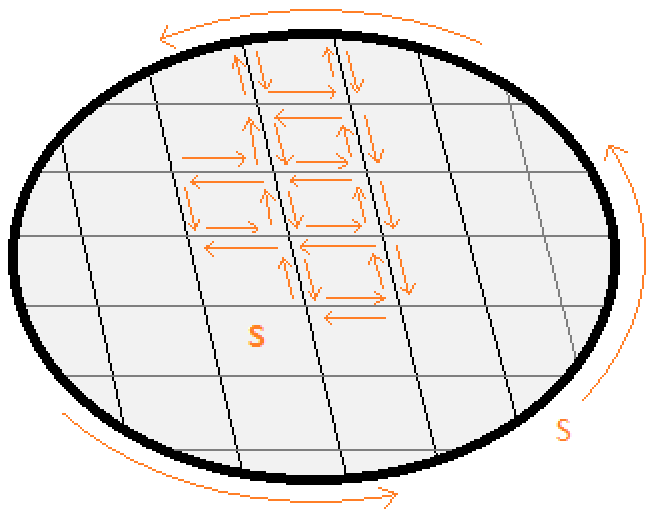

Figure 3: Conversion of the surface integral to the line integral, modified from (Hubbert, 1948). Notice how the interior paths all cancel; however, the exterior paths do not.

Consequently, we can take the line integrals around the exterior periphery of the area of integration, resulting in the following equations.

$$\int\int_S d\theta\, dz = \oint_S \theta\, dz$$

$$g_z = 2G\,\rho \oint \theta\, dz$$

(Talwani, Worzel, & Landisman, 1959) extended this idea by considering the case of an *n*-sided polygon to represent the irregularly-shaped source mass body. The polygon then breaks up the line integral into *n* contributions, each associated with an edge of the polygon. This is visually demonstrated below in Figure 4.

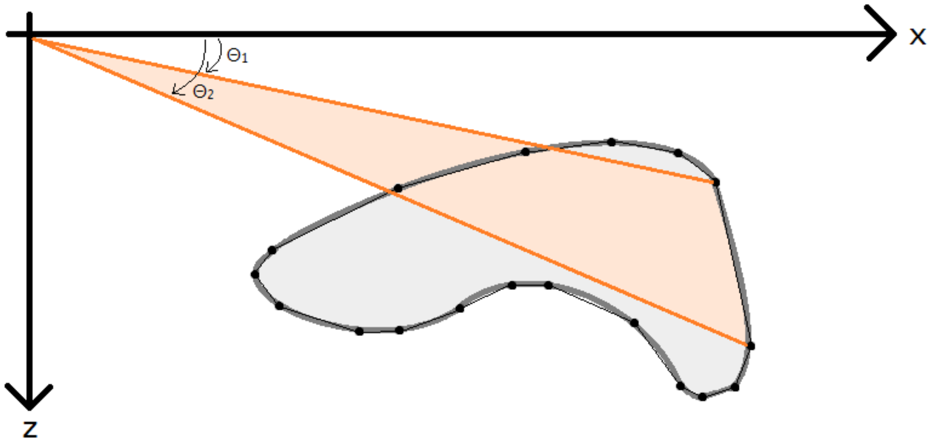

Figure 4: An irregular mass source body (grey) represented as an 18-pt polygon. The points (x_i, z_i) and (x_{i+1}, z_{i+1}) help define Θ_1 and Θ_2 - used in computing the line integral along the ith side of the polygon, modified from (Won & Bevis, 1987).

Given that the origin of the coordinate system is the observation station, the vertical component of the gravity anomaly can be written as follows.

$$\Delta g = 2G\rho \sum_{i=1}^{n} Z_i$$

Z_i above represents the line integral along the i^{th} edge of the polygon. (Talwani, Worzel, & Landisman, 1959)'s implementation uses many trigonometric functions which reduce computational efficiency. (Grant & West, 1965) showed that the expression for Z_i can be formulated by referring more to the vertex coordinates $\{x_i, z_i\}_{i=1,\ldots,n}$ of the polygon.

$$Z_i = A_i \left[(\theta_i - \theta_{i+1}) + B_i \ln \frac{r_{i+1}}{r_i} \right]$$

$$A_i = \frac{(x_{i+1} - x_i)(x_i z_{i+1} - x_{i+1} z_i)}{(x_{i+1} - x_i)^2 + (z_{i+1} - z_i)^2}$$

$$B_i = \frac{z_{i+1} - z_i}{x_{i+1} - x_i}$$

$$r_i^2 = x_i^2 + z_i^2$$

$$r_{i+1}^2 = x_{i+1}^2 + z_{i+1}^2$$

2.5D and 2.75D Modeling was also performed for geologic units known to have limited extents in the *y*-direction (including surface basalts, dikes, etc.). The software permitted the NEOS team to enter their extents in the positive and negative *y*–directions. The following Figure 7 visually shows the differences between 2D, 2.5D, and 2.75D modeling[2].

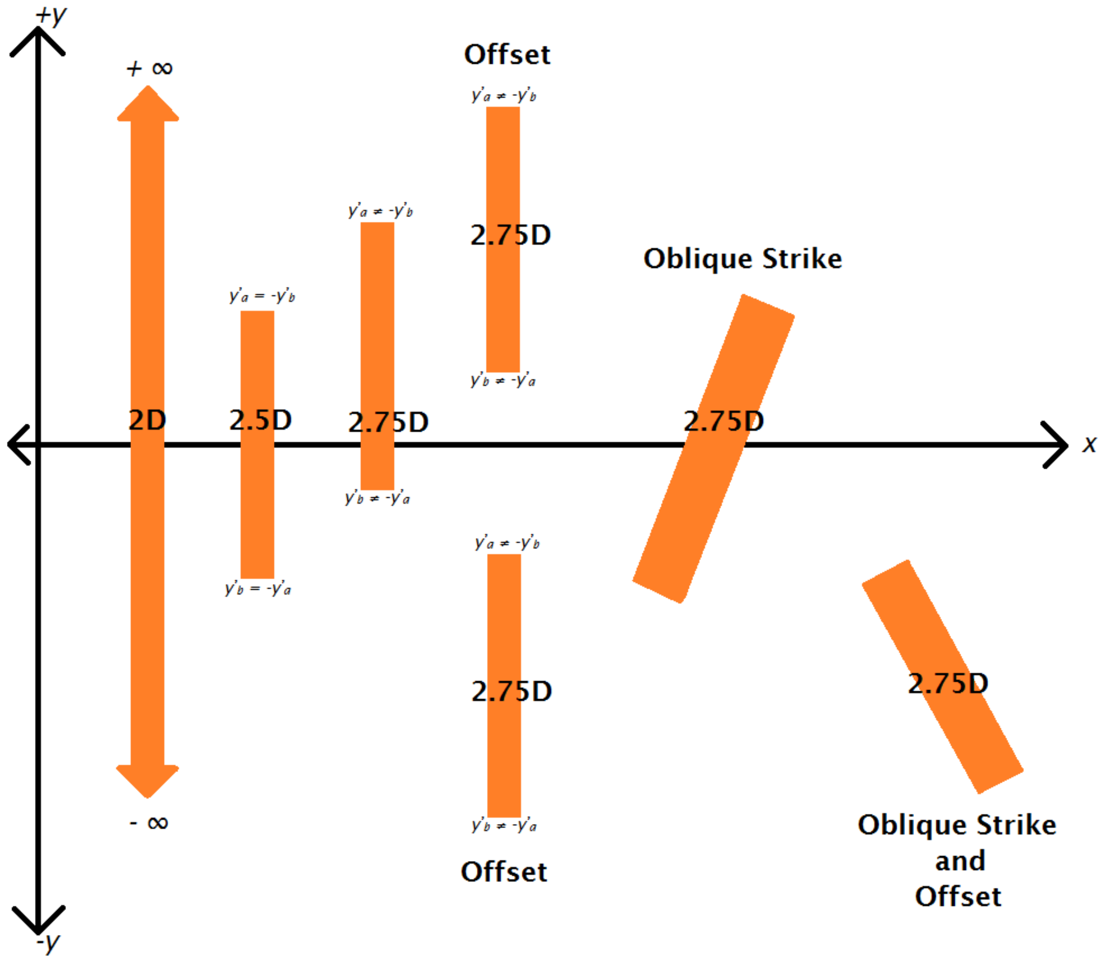

Figure 5: Geometric attributes of elongated bodies in a 2D, 2.5D, and 2.75D sense, modified from (Hinze, Von Frese, & Saad, 2013).

The mathematics behind 2.5D and 2.75D modeling are beyond the scope of this report. (Rasmussen & Pedersen, 1979) and (Hinze, Von Frese, & Saad, 2013) provide good foundations for the theory of these applications.

The gravity data misfit within GM-SYS is defined as the root mean squared (RMS) error given by the following equation.

$$Error_{RMS} = \sqrt{\left(g_{z,meas} - g_{z,calc}\right)^2}$$

[2] It is important to note that 2.5D and 2.75D actually refer in reality to 3D bodies with 3D gravitational potential and vector components.

Where $g_{z,meas}$ is the observed data point, and $g_{z,calc}$ is the calculated data point (the forward problem). The NEOS team also employed 2D Inverse Modeling by inverting the density of a selected block(s), and the *(x,z)* point(s) outlining the blocks.

Once the NEOS team was happy with the forward models and the RMS errors observed, some inverse modeling was applied to the density and susceptibility parameters of various bodies. Where applicable, the location of some of the body polygon vertices were inverted in the *x* and *z* directions. This allowed for a better fit of the data, and higher confidence in the model.

Inverse modeling within GM-SYS is largely based on (Marquardt, 1963) which devised an algorithm for using least-squares to estimate nonlinear parameters (such as those we observe with magnetic and gravity modeling). The algorithm is similar to the Taylor Series method and the Gradient method – combining their best features and avoiding their limitations. The inverse problem can be states as follows.

$$g_{v,calc} = f(x_1, x_2, \dots, x_m;\ \beta_1, \beta_2, \dots, \beta_k)$$

$$= f(\boldsymbol{x}, \boldsymbol{\beta})$$

Where x_1, x_2, …, x_m are independent variables not to be changed during the modeling. β_1, β_2, … , β_k are the parameters in question, which fit the data. The goal of inverse modeling is to approximate **β**. To do this, the model is iteratively adjusted such that the data misfit decreases for each iteration. The data misfit is defined below[3].

$$\varphi = \sum_{i=1}^{n} \left[g_{z,meas} - g_{z,calc} \right]^2$$

(Marquardt, 1963) notes that the contours of constant φ are ellipsoids when *f* is linear; however, those contours are distorted according to the severity of nonlinearity of *f*. The Taylor Series method tries to take advantage of this by linearizing the model. The Taylor Series method is described below.

$$\langle g_{v,calc}(\boldsymbol{X_i}, \boldsymbol{b} + \boldsymbol{\delta_t}) \rangle = f(\boldsymbol{X_i}, \boldsymbol{b}) + \sum_{j=I}^{k} \left(\frac{\partial f_i}{\partial b_j} \right) (\delta_t)_j$$

$$\langle \boldsymbol{g_{v,calc}} \rangle = \boldsymbol{f_0} + \boldsymbol{P}\boldsymbol{\delta_t}$$

The angled brackets above distinguish the linearized model (as opposed to the actual nonlinear model). β is replaced by **b**, where the converged value of **b** approximates β through least-squares. $\boldsymbol{\delta_t}$ is a small correction vector applied to **b**,

[3] Note the difference between the RMS Error, which is showed on the 2D model profiles and the data misfit equations (used for inverse modeling).

whose subscript t denotes that it is calculated by the Taylor Series method. Given the predicted data misfit $\varphi = \sum_{i=1}^{n} \left[g_{v,meas} - \langle g_{v,calc} \rangle \right]^2$ and the equation above depends linearly on $\boldsymbol{\delta}_t$, $\boldsymbol{\delta}_t$ can be found by the standard least-squares method by setting $\frac{\partial \langle \varphi \rangle}{\partial \delta_j} = 0$ for all j and solving the following.

$$\boldsymbol{A\delta_t} = \boldsymbol{g}$$

$$\boldsymbol{A} = \boldsymbol{P}^T \boldsymbol{P}$$

$$\boldsymbol{P}^T = \left(\frac{\partial f_i}{\partial b_j} \right), i = 1,2, \dots, n; j = 1,2, \dots, k$$

$$\boldsymbol{g} = \left(\sum_{i=I}^{n} (Y_i - f_i) \frac{\partial f_i}{\partial b_j} \right), j = 1,2, \dots, k$$

$$= \boldsymbol{P}^T (\boldsymbol{Y} - \boldsymbol{f_0})$$

Often it is required to correct **b** by only a fraction of $\boldsymbol{\delta}_t$ in order to avoid divergence. Otherwise the extrapolation may extend beyond the region where *f* can adequately be linearized. The Gradient method by contrast simply calculates the correction vector using the current iterations data misfit negative gradient, shown below.

$$\boldsymbol{\delta_g} = -\left(\frac{\partial \varphi}{\partial b_1}, \frac{\partial \varphi}{\partial b_2}, \dots, \frac{\partial \varphi}{\partial b_k} \right)^T$$

Very slow convergence for the Gradient method is frequent due to the poor conditioning of φ. As with the Taylor Series method, it is also necessary to control the step size to avoid divergence.

The modified method which is employed by GM-SYS included the advantages of both the Taylor Series and Gradient methods, while avoiding their disadvantages. The Method of Lagrange Multipliers is employed to modify $\boldsymbol{A\delta_t} = \boldsymbol{g}$ to

$$(\boldsymbol{A} + \lambda \boldsymbol{I})\boldsymbol{\delta_0} = \boldsymbol{g}$$

Where *I* is the identity matrix, $\lambda \geq 0$ is the Lagrange multiplier and is arbitrary. $\boldsymbol{\delta}_0$ then exists and minimizes $\langle \varphi \rangle$ on a sphere with radius $||\boldsymbol{\delta}||$ satisfying $\|\boldsymbol{\delta}\|^2 = \|\boldsymbol{\delta_0}\|^2$. A stationary point is required for the Lagrange function. To find the minimum, its derivatives (shown below) must all be zero.

$$u(\boldsymbol{\delta}, \lambda) = \|\boldsymbol{Y} - \boldsymbol{f_0} - \boldsymbol{P\delta}\|^2 + \lambda(\|\boldsymbol{\delta}\|^2 - \|\boldsymbol{\delta_0}\|^2)$$

$$\frac{\partial u}{\partial \delta_1} = \frac{\partial u}{\partial \delta_2} = \cdots = \frac{\partial u}{\partial \delta_k} = 0, \qquad \frac{\partial u}{\partial \lambda} = 0$$

Taking the respective derivatives and setting them to zero gives the following.

$$0 = -[\boldsymbol{P}^T(\boldsymbol{Y} - \boldsymbol{f_0}) - \boldsymbol{P}^T\boldsymbol{P}\boldsymbol{\delta}] + \lambda\boldsymbol{\delta}$$

$$\mathbf{0} = \|\boldsymbol{\delta}\|^2 - \|\boldsymbol{\delta_0}\|^2$$

For a given λ, the following equation satisfies the above solving for **δ**.

$$(\boldsymbol{P}^T\boldsymbol{P} + \lambda\boldsymbol{I})\boldsymbol{\delta} = \boldsymbol{P}^T(\boldsymbol{Y} - \boldsymbol{f_0})$$

$$\boldsymbol{\delta} = (\boldsymbol{P}^T\boldsymbol{P})^{-1}\boldsymbol{P}^T(\boldsymbol{Y} - \boldsymbol{f_0}) - (\boldsymbol{P}^T\boldsymbol{P})^{-1}\lambda\boldsymbol{\delta}$$

Thus an algorithm is constructed (below) for the r^{th} iteration, and is solved for $\delta^{(r)}$. This correction vector is then used to create a new trial vector approximating **β**, which leads to data misfit $\varphi^{(r+1)}$.

$$\left(\boldsymbol{A}^{(r)} + \lambda^{(r)}\boldsymbol{I}\right)\boldsymbol{\delta}^{(r)} = \boldsymbol{g}^r$$

$$\boldsymbol{b}^{(r+1)} = \boldsymbol{b}^{(r)} + \boldsymbol{\delta}^{(r)}$$

It is also important to show that $\|\boldsymbol{\delta}(\lambda)\|^2$ is a continuous decreasing function as $\lambda \rightarrow \infty$. This shows that there is always a sufficiently large $\lambda^{(r)}$ such that $\varphi^{(r+1)} < \varphi^{(r)}$ unless $\mathbf{b}^{(r)}$ already achieves the minimum φ.

$$\boldsymbol{\delta} = \frac{\boldsymbol{r}}{\boldsymbol{C} + \lambda\boldsymbol{I}}$$

$$\|\boldsymbol{\delta}(\lambda)\|^2 = \boldsymbol{g}^T\boldsymbol{S}(\boldsymbol{C} + \lambda\boldsymbol{I})^{-1}\boldsymbol{S}^T\boldsymbol{S}(\boldsymbol{C} + \lambda\boldsymbol{I})^{-1}\boldsymbol{S}^T\boldsymbol{g}$$

$$= \boldsymbol{g}\boldsymbol{g}^T((\boldsymbol{C} + \lambda\boldsymbol{I})^2)^{-1}$$

$$= \sum_{j=1}^{k} \frac{g_j}{\left(C_j + \lambda\right)^2}$$

Where $\boldsymbol{C}=\boldsymbol{S}^T\boldsymbol{A}\boldsymbol{S}$, and $\boldsymbol{S}^T\boldsymbol{S}=\boldsymbol{I}$. This result clearly shows that $\|\boldsymbol{\delta}(\lambda)\|^2$ is a continuous decreasing function of λ such that as $\lambda \rightarrow \infty$, $\|\boldsymbol{\delta}(\lambda)\|^2 \rightarrow 0$ (Morrison, 1960).